

University of Groningen

Dimethyl sulphide

Zemmelink, Hendrik Jan

IMPORTANT NOTE: You are advised to consult the publisher's version (publisher's PDF) if you wish to cite from it. Please check the document version below.

Document Version

Publisher's PDF, also known as Version of record

Publication date:

2003

[Link to publication in University of Groningen/UMCG research database](#)

Citation for published version (APA):

Zemmelink, H. J. (2003). *Dimethyl sulphide: Measuring emissions from the ocean to the atmosphere*. s.n.

Copyright

Other than for strictly personal use, it is not permitted to download or to forward/distribute the text or part of it without the consent of the author(s) and/or copyright holder(s), unless the work is under an open content license (like Creative Commons).

The publication may also be distributed here under the terms of Article 25fa of the Dutch Copyright Act, indicated by the "Taverne" license. More information can be found on the University of Groningen website: <https://www.rug.nl/library/open-access/self-archiving-pure/taverne-amendment>.

Take-down policy

If you believe that this document breaches copyright please contact us providing details, and we will remove access to the work immediately and investigate your claim.

Downloaded from the University of Groningen/UMCG research database (Pure): <http://www.rug.nl/research/portal>. For technical reasons the number of authors shown on this cover page is limited to 10 maximum.

CHAPTER 5

SIMULTANEOUS USE OF RELAXED EDDY ACCUMULATION AND GRADIENT FLUX TECHNIQUES FOR THE MEASUREMENT OF SEA-TO-AIR EXCHANGE OF DIMETHYL SULPHIDE

Abstract-The sea-to-air flux of the biogenic volatile sulphur compound dimethyl sulphide was assessed with the relaxed eddy accumulation (REA) and the gradient flux (GF) techniques from a stationary platform in the coastal Atlantic Ocean. Fluxes varied between 2 and 16 $\mu\text{mol m}^{-2} \text{d}^{-1}$. Fluxes derived from REA were on average $7.1 \pm 5.0 \mu\text{mol m}^{-2} \text{d}^{-1}$, not significantly different from the average flux of $5.3 \pm 2.3 \mu\text{mol m}^{-2} \text{d}^{-1}$ derived from GF measurements. Gas transfer velocities were calculated from the fluxes and seawater DMS concentrations. They were within the range of gas transfer rates derived from commonly used parameterizations that relate gas transfer to wind speed.

5.1 INTRODUCTION

The oceans play a fundamental role in the global climate system on account of their capacity to store and transport heat and absorb and emit trace gases, which affect atmospheric chemistry and radiative transfer. Quantification of the magnitude of trace gas fluxes between the ocean and the atmosphere has been a major research topic in the past decade. However, there still is a large uncertainty in the magnitude of fluxes. This is largely due to the discrepancy that exists between commonly used gas exchange models, with differences up to 100% (Wanninkhof, 1992). These models rely on the assumption that the flux (F) of a gas across the air-water interface is governed by the air-water concentration disequilibrium (ΔC)

$$F_c = k_{\text{gas}} \Delta C \quad (5.1)$$

where k_{gas} is the gas transfer velocity. The gas transfer velocity is usually derived from wind tunnel, radiocarbon, and tracer measurements and related to wind speed and sea surface temperature but not to other environmental parameters that could affect the flux. Ideally, gas transfer velocities would be derived from field measurements of gas fluxes; k_{gas} could then be computed directly and all parameters that affect gas exchange would be included automatically.

Meteorological techniques that are almost routinely used for the measurement of fluxes and deposition velocities of gases and aerosols over terrestrial systems are now being applied to

Chapter 5

the marine environment. The eddy correlation (direct covariance) method is the most direct means of estimating the gas flux *in situ*. Recent experiments have shown that eddy correlation (EC) measurement of carbon dioxide exchange over marine systems are feasible (Edson et al., 1998; Jacobs et al., 1999; McGillis et al., 2001a) and could lead to a better understanding of environmental parameters that affect the exchange of gases between the ocean and the atmosphere. The EC technique has been identified as a promising tool for the measurement of carbon dioxide fluxes at the sea-air interface (Houghton, 2001). However, the application of EC is limited to trace gases such as CO₂ and H₂O for which fast response sensors exist. Even so, fluxes of the main species of interest, CO₂, are often at the limit of detection (McGillis et al., 2001a).

The biogenic gas dimethyl sulphide (DMS) is different because it exhibits a strong concentration gradient between the ocean and the air so fluxes are always evident. In the atmosphere, DMS is oxidized in about 1 day, which allows the determination of the flux by micrometeorological measurements, typically conducted over time spans of 20 to 60 minutes. These characteristics make DMS a useful model gas for process studies of gas exchange between the ocean and the atmosphere. New progress in gas analysis, based upon fast response chemiluminescence detectors and mass spectrometry allows the measurement of DMS concentrations in time spans less than a second, in principle allowing DMS flux observations based on the EC technique (Jodwalis and Benner, 1995; Spicer et al., 1996). However, EC of DMS fluxes has never been realized, as yet, and intercalibration with different analytical methods is required before the EC method for DMS fluxes can be applied with confidence. Unfortunately, the fast detector response required for EC is beyond the present capability of gas chromatographic systems that are used to measure DMS concentrations. Meteorological techniques that do not rely on fast response sensors have been successfully applied for the measurement of trace gas fluxes between terrestrial ecosystems and the atmosphere. This Chapter focuses on the application of two such techniques, the gradient flux (GF) and relaxed eddy accumulation (REA) techniques, for the measurement of DMS emissions over the marine environment.

5.2 MATERIALS AND METHODS

5.2.1 Relaxed eddy accumulation.

Businger and Oncley (1990) examined sets of raw EC measurements of humidity, and temperature. They noted that if measurements of temperature and humidity were segregated according to the sign of the vertical wind speed w (m s^{-1}), the flux was proportional to the product of the standard deviation of the vertical wind speed, σ_w (m s^{-1}), and the average humidity or temperature difference between updrafts and downdrafts. Thus

$$F_c = \beta_0 \sigma_w (\bar{C}_u - \bar{C}_d) \quad (5.2)$$

where \bar{C} is the mean concentration in the upward and downward moving eddies. They found that the coefficient of proportionality, β_0 , is relatively insensitive to atmospheric stability; it is close to 0.6. This technique, "relaxed eddy accumulation" (REA), involves sampling air into updraft and downdraft reservoirs at a constant flow rate, rather than proportionally to the vertical wind speed, w , as is the case in the true eddy accumulation methodology. Often, a threshold wind velocity is used for switching the valve that directs the samples into the upward or downward collection reservoirs. This "deadband approach" has the advantage of increasing the concentration difference between the two reservoirs because sampling is biased toward larger eddies (those with sufficient vertical velocity to exceed the threshold) which tend to move air farther along the vertical concentration gradient. The increase in concentration difference must be balanced by a decrease in β_0 . Businger and Oncley (1990) and later Pattey et al. (1993) found an exponential decrease in β_0 with increasing deadband size (w_0)

$$\beta = \beta_0 \exp(-0.75 w_0 / \sigma_w) \quad (5.3)$$

Equation 5.3 is derived from Businger and Oncley (1990) who defined, for practical reasons, the deadband velocity $2w_0$ around $\bar{w} = 0$. For this study a fixed deadband velocity of $\pm 0.03 \text{ m s}^{-1}$ has been used.

Configuration. Relaxed eddy accumulation (REA) permits collection of air in two configurations. The first configuration is used to collect samples in traps that specifically

Chapter 5

adsorb the compounds of interest while other compounds pass through the traps unretained. With these “flow through reservoirs” the gases are directly concentrated during the sampling period (Nie et al., 1995). The second configuration is used to collect samples in reservoirs with a single inlet, such as bags (Pattey et al., 1993). Zemmeling et al. (2002a) found that DMS remains stable for at least a week in Tedlar collection bags. They concluded that the second configuration was more reliable for the measurement of DMS fluxes. In this configuration the pump has to be located upstream of the collection reservoirs. This might increase the danger of DMS retention within the sampler and pump, or contamination of the sampled air. However, tests indicated that the materials used in the REA system (Teflon and Stainless Steel) were inert to DMS (results not shown).

Design of the REA sampler (Figure 5.1).

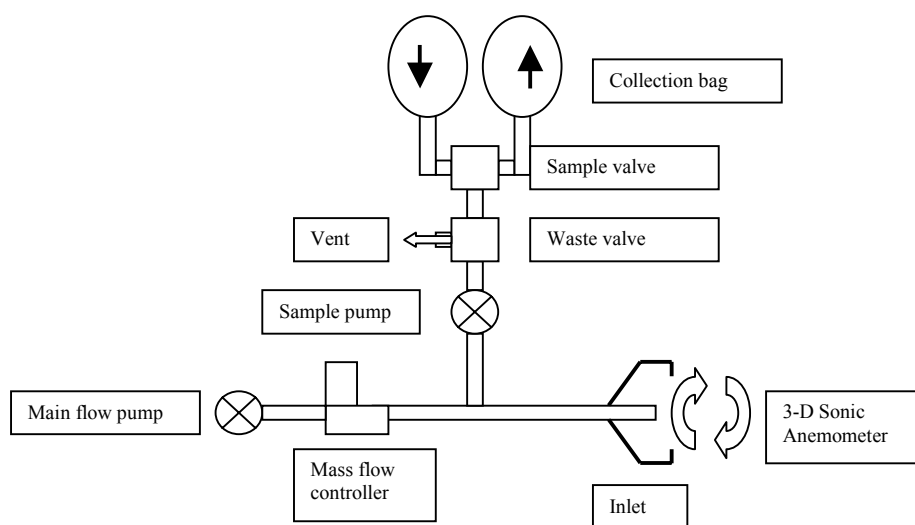


Figure 5.1. Schematic of the relaxed eddy accumulation system. See text for more details.

The sampling inlet was located near a "3-D" sonic anemometer ("Applied Technology" Inc.), which was capable of measuring the wind speed at a frequency of 10 Hz. The main flow of air was transported through 0.4 cm diameter Teflon tubing at a flow rate of 7.5 l min^{-1} . The flow rate of the main flow was kept constant using a mass flow controller. The tubing diameter and the sample flow must be selected to ensure turbulent, not laminar flow in the main flow line. Laminar flow would lead to an attenuation of turbulent fluctuations and could mix updraft and downdraft

air before they are segregated (Massman, 1991; Suyker and Verma, 1992; Rannik et al., 1997). The Reynolds number for the flow in a tube is

$$Re = d_t U_t \nu^{-1} \quad (5.4)$$

where d_t (m) is the inside tube diameter, U_t ($m s^{-1}$) is the flow velocity in the tube, and ν ($m^2 s^{-1}$) is the viscosity of air. Re should be larger than 2300 for turbulent tube flow. The flow rate and tube diameter used gave a Re number of 2635. A sample of $300 ml min^{-1}$ was drawn from the main flow near the system inlet using a diaphragm sample pump. The sample pump was connected downstream in series to two fast response (20Hz) 3-way valves. The first of these (the waste valve) either vents the air when the vertical wind speed does not exceed the threshold velocity, or leads the air to the second valve (the sample valve) that distributes the air to the updraft or downdraft collection reservoirs depending on the sign of the wind velocity.

REA operating procedure. A 5-minute running average at the start of each sampling period was used to compute the mean of the vertical wind speed, \overline{w} . During this initialization period the air is vented by the first valve. During the sampling, each new reading of the actual vertical wind velocity, w , is used to calculate the difference between \overline{w} and w . When this exceeds the threshold value, the waste valve sends the air to the sample valve so the air is distributed to the two bags according to the sign of the actual wind velocity. The switching signal is delayed to allow the air sample from the eddy that has triggered the switch to arrive at the valves.

5.2.2 Gradient flux.

From a series of experiments conducted over the Plains of Kansas (Businger et al., 1971), a number of semi-empirical relations has been deduced. These relations describe the exchange processes in a relatively simple manner. The most commonly used model is based on the flux-gradient theory, which allows an estimation of the flux from mean concentration gradients in the vertical direction z in the atmospheric boundary layer

$$F = \frac{u_* k}{\Phi(z/L)} \frac{\partial C}{\partial \ln z} \quad (5.5)$$

Chapter 5

where u_* (m s^{-1}) is the friction velocity (derived in this study from the momentum flux, calculated from the correlation between the horizontal (u) and vertical (w) wind velocities, k is the von Karman constant (0.40), $\frac{\partial C}{\partial \ln z}$ is the change of concentration (C) with the natural logarithm of height (z), and $\Phi(z/L)$ is the Monin-Obukhov stability function. Empirical relationships for stability functions have been proposed by many authors (e.g. Dyer and Hicks, 1970; Paulson, 1970; Businger et al., 1971; Dyer, 1974; Högström, 1988; Edson and Fairall, 1998). In this study we used the following relations (Dyer and Hicks, 1970): in neutral atmospheric stratification $\Phi(z/L) = 1$, in unstable conditions $\Phi(z/L) = (1 - 16\zeta)^{-1/2}$, and in stable conditions $\Phi(z/L) = 1 + 5\zeta$. Here ζ is the dimensionless ratio of measurement height (z) to the Monin-Obukhov length (L)

$$\zeta = \frac{z}{L} \quad \text{with} \quad L = \frac{\bar{\theta} u_*^3}{k g F_\theta} \quad (5.6)$$

where θ is the virtual temperature, g is the acceleration due to gravity, and F_θ is the buoyancy flux (derived from eddy correlation measurements).

Design of the GF sampler (Figure 5.2).

Air from a series of inlets was sampled through 25 m of Teflon tubing to Vac-U-Chamber airtight boxes (SKC Inc.), into which 10-liter Tedlar bags were placed for sample accumulation (Figure 5.2). Several Vac-U-Chamber boxes could be evacuated with a single diaphragm pump, and a 3-way valve on each box allowed switching from purging the tubing to collecting air samples (Figure 5.2, bottom). A ballast chamber between the pump and the boxes ensured a steady flow. A metering valve between the pump and the ballast chamber was used to control the sample collection rate.

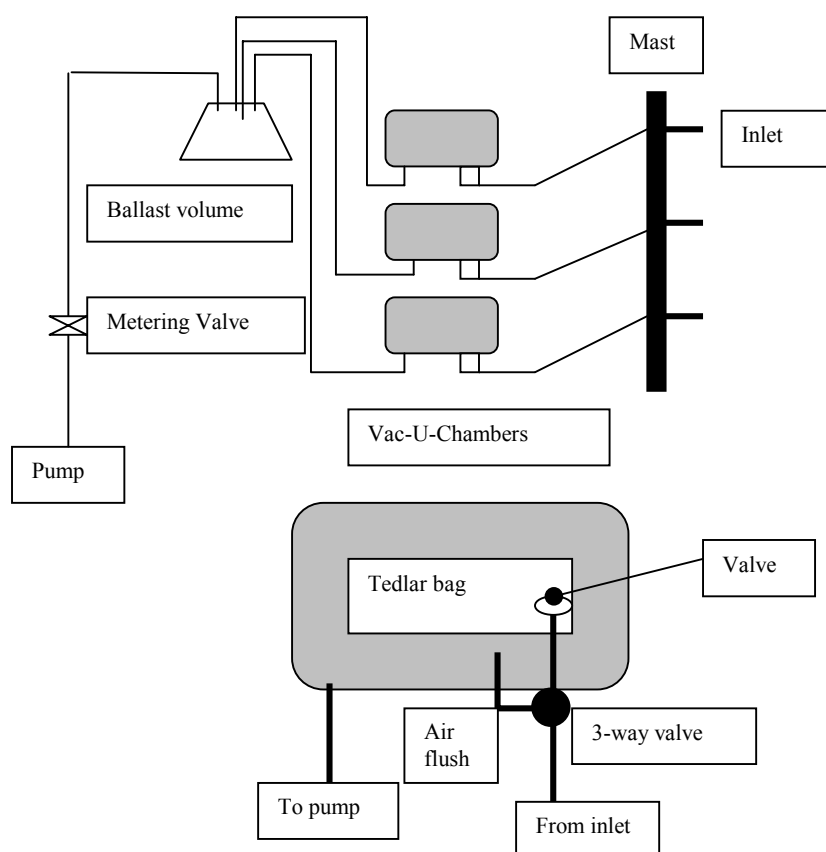


Figure 5.2. Schematic of the gradient flux system. See text for more details.

5.2.3 Collection and analysis of air samples.

Measurements were conducted on three days in June 2000 from a dock extending 20 m off shore near Woods Hole, MA (41.2°N, 70.8°W). Air was typically sampled for 30 min at a flow rate of $\sim 300 \text{ ml min}^{-1}$ and collected in Tedlar bags for both techniques. The inlets of the GF system were mounted to the mast of a small catamaran riding on the water surface, at elevations of approximately 0.4, 1.5, and 2 m; the REA inlet was at an elevation of 1.75 m. Oxidants were removed by a KI oxidant scrubber (Kittler et al., 1992) placed in the GF inlets and close to the collection reservoirs of the REA system. Sampled air was stored in the bags and brought to the laboratory for further analysis. In the laboratory the air was dried over a cold finger, after which the DMS was concentrated onto 240 mg Tenax TA, with both the cold finger and the Tenax trap cooled to -15°C . (Storage of bags at equal temperature and drying the air removes the effect of

Chapter 5

density fluctuations on the gas analysis). The flow rate during drying and trapping was 300 ml min⁻¹ (using a mass flow controller), with 1 liter of air sufficient for an accurate determination of the amount of DMS. After concentration, the temperature of the Tenax trap was increased to 180°C to desorb the retained DMS into a Sievers gas chromatograph equipped with a sulfur chemiluminescence detector (detection limit ~5x10⁻¹³ mol). Samples were analyzed in triplicate from each bag.

Water samples were taken upwind of the meteorological measurement systems for the analysis of DMS in surface water. At least one water sample was taken during every flux measurement. During the third day the surface water was sampled every 50 meters upwind of the measurement systems to 200 meters in order to measure the variability of DMS in the source area of the flux. On return to the laboratory, 4 ml of water were purged with nitrogen at a flow rate of 120 ml min⁻¹ for five minutes. The DMS-containing gas was dried in a cold finger, and the DMS was trapped on cold Tenax and analyzed as described above.

Fluxes were calculated by combining Equations 2 and 3 for REA, and 5 and 6 for GF. Corrections for solubility (Dacey et al., 1984) were on the order of 3% and considered to be negligible for the calculation of the absolute flux and transfer velocities. Transfer velocities were derived using Equation 5.1, neglecting the effect of the air side control of the flux (McGillis et al., 2000). Transfer velocities were normalized to seawater at a temperature of 20°C by means of the Schmidt number (Sc) dependence suggested by Wanninkhof (1992)

$$k_{660} = k_{\text{gas}} (\text{Sc}_{\text{DMS}}/660)^{1/2} \quad (5.7)$$

where Sc_{DMS} is the Schmidt number of DMS calculated following Saltzman et al. (1993).

5.2.4 Wind induced errors.

Vertical wind bias. Averaged over the sampling interval, the mean vertical wind velocity should ideally be zero. When the average vertical wind velocity significantly deviates from zero, the total flux from REA is made up of the sum of the horizontal flux (advective flux) and the vertical eddy flux. In eddy correlation systems, any error introduced this way can be corrected mathematically by rotation of the reference frame of the measurement system to match the mean wind stream lines after the sampling is concluded (Kaimal and Finnigan, 1994). Unfortunately this correction is impossible for REA, where the collection of air is based on real-time velocity

measurements. In order to minimize the effect of the advective flux, samples with $\overline{w} > 1\% * \overline{u}$ were rejected. The 1% level is an arbitrary choice and resulted in a rejection of 15% of the total number of measurements.

5.3 RESULTS AND DISCUSSION

Environmental conditions varied over the time span of the experiments. Average wind speed at 2 m elevation ranged from 4 to 6.5 m sec⁻¹, water temperature increased from 17 to 19.3°C, and air temperature increased from 16 to 24°C between June 1 and June 24, 2000. The DMS concentration in the water increased from 2.7 nmol l⁻¹ to 6.1 nmol l⁻¹. Water samples taken in the upwind fetch of the measurements revealed spatial homogeneity of aqueous DMS concentrations to within 16%. A thorough description of environmental characteristics that may have influenced the micrometeorological measurements (sea state; thickness of the constant flux layer) was not within the scope of this study but should be taken into account in future work.

Fluxes. Measured fluxes varied between 2 and 16 $\mu\text{mol m}^{-2} \text{d}^{-1}$ (Figure 5.3), with fluxes derived from REA on average 7.1 \pm 5.03 $\mu\text{mol m}^{-2} \text{d}^{-1}$ and fluxes derived from GF measurements 5.3 \pm 2.3 $\mu\text{mol m}^{-2} \text{d}^{-1}$. Linear regression of simultaneous fluxes derived from REA vs. GF yields $\text{REA} = 1.33 * \text{GF}$ ($R^2 = 0.33$) when forced through zero. Exclusion of the results at 4.4 m s⁻¹, which showed a large discrepancy between the two measurements, yields a slope of 1.1 and $R^2 = 0.68$ (exclusion of this measurement from further analysis was, however, not justified). Although the data set is limited, statistics showed that the average fluxes derived from both methods were not significantly different ($p < 0.05$).

The reproducibility of replicates was sometimes low (up to 20% difference, e.g. replicates at 0.4 meters in the upper profile in Figure 5.4) but often reasonable (within 10%); the high uncertainty was due to problems with the cooling of the GC analytical trap. Error bars in Figure 5.3 from fluxes derived with the REA method represent maximum and minimum fluxes that could be calculated from the triplicate analysis in the updraft and downdraft collection reservoirs. Error bars of the fluxes derived from the GF technique represent the 95% confidence interval of the linear regression through $dC/d\ln z$ (Figure 5.4). The flux derived from the two profiles shown was 7.34 \pm 2.5 $\mu\text{mol m}^{-2} \text{d}^{-1}$ (top profile) and 4.36 \pm 4.8 $\mu\text{mol m}^{-2} \text{d}^{-1}$ (bottom profile). Hence, the error bars in Figure 5.3 represent the uncertainty due to the replicate analysis only.

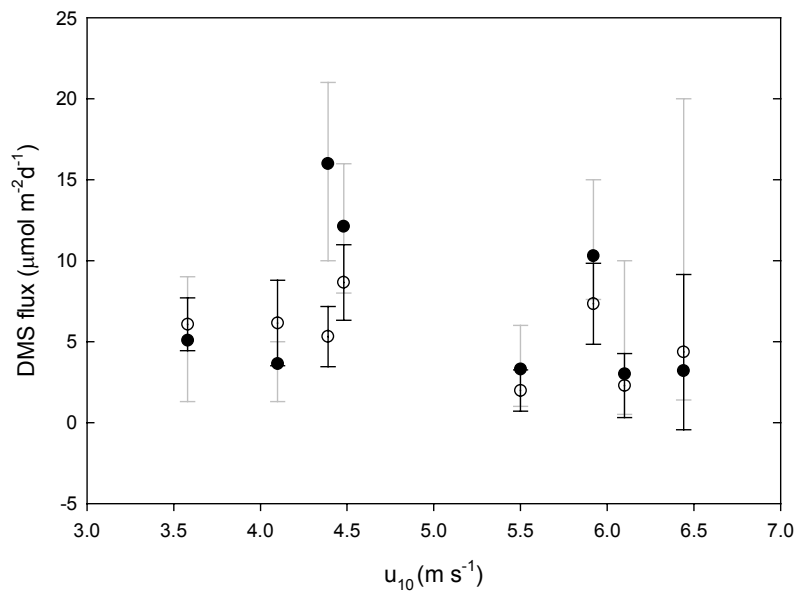
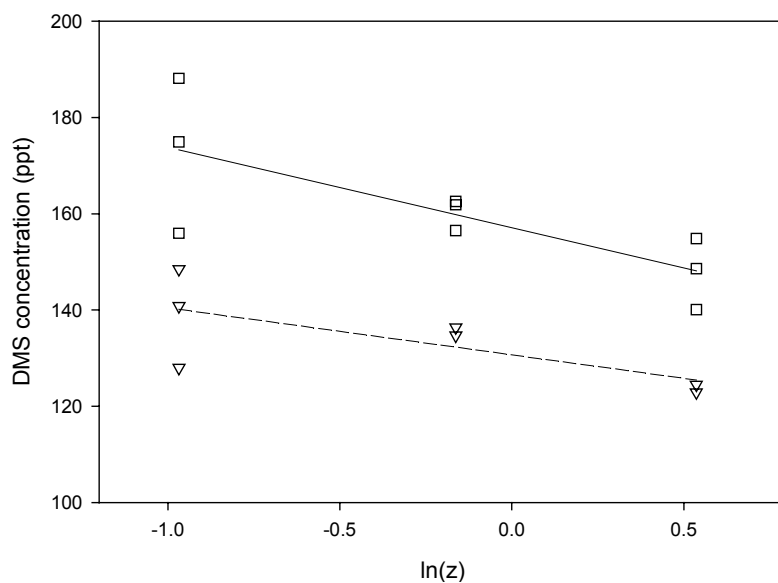


Figure 5.3. DMS flux ($\mu\text{mol m}^{-2} \text{d}^{-1}$) versus wind speed at ten meter elevation (m s^{-1}) derived from REA (solid circles) and GF (open circles) measurements. Error bars of the REA measurements represent the lowest and highest fluxes derived from one pair of samples. Error bars for GF represent the 95% confidence interval of the linear regression through the concentration gradient profiles (Figure 5.4).



(Figure 5.4)

Sources of error. In contrast to EC, which is generally accepted as an accurate measurement of the flux, REA and GF are techniques that rely on empirically derived functions, of which the application in the marine environment is relatively new. Hence little is known about their applicability for the measurement of DMS fluxes. Although good results have been obtained from REA measurements over terrestrial systems, the universality of this technique remains an open question. Two issues should be taken into consideration to determine the accuracy of REA: how reliable is the approximation of β , and how accurate is the measurement of w which will determine the size of σ_w (the noise level of the 3-D sonic anemometer is sufficiently low to have no effect on w and σ_w). EC simulations of REA over terrestrial systems by Businger and Oncley (1990) and more recently by Andreas et al. (1998) showed that β varies between 0.48 and 0.65 and is relatively insensitive to atmospheric stability. Recent studies suggest that this also applies to oceanic environments (Chapter 6). In this study values of β were calculated by using Equation 5.3. They varied between 0.55 and 0.57, similar to average values found in the literature that yield numbers around 0.56-0.58 (Baker, 1992; Pattey et al., 1993; Beverland et al., 1996; Katul et al., 1996). The accuracy of the REA system can of course be affected by technical factors. Among them is the response time of the sampling system to changes in the vertical wind direction. There are several components to this type of error: 1) high frequency changes (faster than 10 Hz) in the vertical wind velocities that are missed by the sonic anemometer response, and 2) the time lag or other imprecision between changes in the vertical wind direction and the switching of valves that distribute the samples between the collection reservoirs. However, the higher fluxes derived from the REA measurements are not likely to be caused by this type of error since this is more likely to result in an underestimation of the gas flux because updraft air will be sampled as downdraft air and vice versa.

Figure 5.4. Two profiles showing the concentration gradient of DMS (ppt) versus $\ln(z)$ (m). Lines represent the best fit through the profiles. Estimated fluxes from these profiles are 7.34 ± 2.5 and 4.36 ± 4.8 ($\mu\text{mol m}^{-2} \text{d}^{-1}$) for the top and bottom profiles respectively (error bars show the 95% confidence interval of the slope). The high uncertainty at 0.4 meter was due to problems with the cooling of the GC analytical trap.

Chapter 5

Most of the proposed stability functions for the gradient method differ only in the values of the constants used. As yet there is no function that should be preferred for use over the sea surface. In addition, the GF method relies on EC measurements of momentum and latent heat fluxes (Equation 5.5), the accuracy of which is typically on the order of 10-30%. In Figure 5.3, the uncertainty of the flux is expressed in terms of the 95% confidence interval of the linear regression through all measured concentrations. Another approach is to compare the flux that is calculated from the concentrations measured at the two upper and two lower heights. This resulted in fluxes of 6.9 to 7.82 $\mu\text{mol m}^{-2} \text{d}^{-1}$ (top profile) and 1.98 to 7.64 $\mu\text{mol m}^{-2} \text{d}^{-1}$ (bottom profile). The lower pair of sampling inlets gave an underestimation of the flux compared to the higher pair. This implies that the profile is not properly described by Equation 5.4, which assumes a log-linear relation between C and z. Fuentes et al. (1996) discuss the effect of the size of the atmospheric sublayers on gradient measurements over tall vegetation. Two sublayers are distinguished: a constant flux layer (the inertial sublayer), in which the flux-gradient relationships are valid, and a lower roughness sublayer immediately above the surface where the validity of the relationships is uncertain due to the proximity of roughness elements. Cellier and Brunet (1992) and Pattey et al. (1999) have shown that sampling inlets located in the roughness sublayer caused a significant underestimation of the flux. Hence, Equation 5.4 does not properly describe profile relationships close to the surface and requires that measurements be made well above the roughness length, z_0 . The roughness of the sea surface can be calculated following Maat et al. (1991): $z_0 = 0.8 u_*^3 / v_p g$ where v_p (m s^{-1}) is the phase speed of the waves and g (m s^{-2}) is the acceleration due to gravity. However, v_p was not measured in this study and an estimation of z_0 can be made following Charnock (1955): $z_0 = 0.018 u_*^2 / g$ which in contrast to the Equation of Maat et al. (1991) does not take the effect of wave age on the roughness of the sea surface into account. The roughness length during the measurements was $\sim 1.4 \times 10^{-4}$ m, well below the lowest sampling inlet (0.38 m) and could not have affected our measurements.

Transfer velocities. The transfer coefficient, k_{gas} is usually derived from parameterizations that relate gas transfer rates to short-term measurements of wind speed as suggested by Liss and Merlivat (1986) and Wanninkhof (1992). The first is based on a wind speed extrapolation from a tracer release experiment with a time scale of 1-2 days and the latter is based on mean wind speeds and the global ^{14}C budget. The application of both parameterizations is confined to the computation of large-scale averaged fluxes while the measured turbulent fluxes represent local processes that occur on time scales of an hour or less. Figure 5.5 shows the

transfer velocities derived from the field measurements, the parameterizations as suggested by Liss and Merlivat (1986) and Wanninkhof (1992), and the relationship between gas transfer and wind speed as suggested by Jacobs et al. (1999) and McGillis et al. (2001a). The Jacobs et al. model is based on half-hourly EC measurements of CO₂ fluxes.

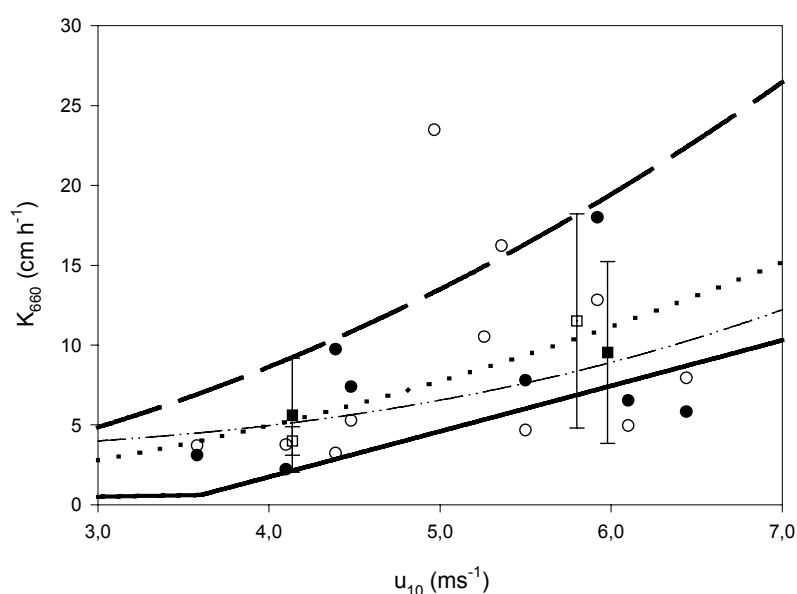


Figure 5.5. Gas transfer velocities (cm h^{-1}) versus wind speed at 10 m elevation (m s^{-1}) derived from REA measurements (solid circles) and GF measurements (open circles). Error bars on the individual measurements are not shown but are proportional to the error bars in Figure 5.2. Squares represent the average transfer velocities above and below $U = 5 \text{ m s}^{-1}$; error bars are 1 standard deviation from the mean. Also shown are the gas transfer relationships as proposed by Liss and Merlivat (1986, solid line) and Wanninkhof (1992, dotted line) and the meteorologically derived gas transfer relationships from Jacobs et al. (1999, dashed line) and McGillis et al. (2001a, dashed-dotted line).

Transfer velocities derived from the DMS measurements fall within the discrepancy between the proposed models. The large scatter is in agreement with results of Jacobs et al. (1999) and might indicate that processes other than wind speed affect the flux, or affect the applicability of the REA or GF methods. However, the paucity of field measurements of trace gas exchange, specifically of DMS, hampers insight into processes that cause the observed scatter. Bin-averaged

Chapter 5

transfer velocities for wind speeds $< 5 \text{ m s}^{-1}$ and $> 5 \text{ m s}^{-1}$ show that transfer velocities based on short-term measurements of wind speed are best represented by the model proposed by Wanninkhof (1992); the model proposed by Liss and Merlivat (1986) would result in an underestimation of DMS fluxes. However, given the limited data set it is difficult to compare the transfer velocities derived from these field measurements with the large-scale model parameterizations.

Outlook. In the future further intercalibration of techniques, in combination with a detailed study of meteorological conditions and physical processes in the fetch areas of the measurement systems, is necessary in order to apply the techniques with confidence. The main goal of this study was to test the feasibility DMS flux measurements by the REA and GF methods; we did not aim at a more thorough study of processes that could affect the flux or the measurement techniques. These aspects will be considered in the following chapters that describe experiments conducted in conditions representative of the open ocean.

5.4 CONCLUSIONS

Our experiments show that the measurement of sea-to-air DMS fluxes is possible with the gradient flux and relaxed eddy accumulation techniques. Comparison of fluxes and transfer velocities derived with the GF and the REA system reveals that results obtained by both methods agree quite well. Both techniques are a promising tool for process studies of air-sea gas exchange. Since the completion of these experiments, we have performed further REA and GF studies of DMS flux and k_{gas} on the FAIRS and GasEx-2001 cruises. The results of these studies will be reported in Chapter 6,7 and 8.